

## MIT Open Access Articles

*A comparison of nanoparticle-antibody conjugation strategies in sandwich immunoassays*

The MIT Faculty has made this article openly available. **Please share** how this access benefits you. Your story matters.

**Citation:** Tam, Justina O. et al. "A comparison of nanoparticle-antibody conjugation strategies in sandwich immunoassays." *Journal of Immunoassay and Immunochemistry* 38, 4 (January 2017): 355-377 © 2017 Taylor & Francis

**As Published:** <http://dx.doi.org/10.1080/15321819.2016.1269338>

**Publisher:** Informa UK Limited

**Persistent URL:** <https://hdl.handle.net/1721.1/126437>

**Version:** Author's final manuscript: final author's manuscript post peer review, without publisher's formatting or copy editing

**Terms of use:** Creative Commons Attribution-Noncommercial-Share Alike





Published in final edited form as:

*J Immunoassay Immunochem.* 2017 ; 38(4): 355–377. doi:10.1080/15321819.2016.1269338.

## A Comparison of Nanoparticle-Antibody Conjugation Strategies in Sandwich Immunoassays

Justina O. Tam<sup>§</sup>, Helena de Puig<sup>^</sup>, Chun-wan Yen<sup>§</sup>, Irene Bosch<sup>‡</sup>, Jose Gómez-Márquez<sup>%</sup>, Charles Clavet<sup>§</sup>, Kimberly Hamad-Schifferli<sup>#, ^</sup>, and Lee Gehrke<sup>+, ‡</sup>

<sup>§</sup> Winchester Engineering and Analytical Center, U.S. Food and Drug Administration, Winchester, MA USA 01890

<sup>^</sup> Dept. of Mechanical Engineering, Massachusetts Institute of Technology, Cambridge, MA USA 02139

<sup>‡</sup> Institute for Medical Engineering and Science, Massachusetts Institute of Technology, Cambridge, MA USA 02139

<sup>%</sup> MIT Little Devices Lab and the MIT-SUTD International Design Centre, Massachusetts Institute of Technology, Cambridge, MA USA 02139

<sup>#</sup> Dept. of Engineering, University of Massachusetts Boston, Boston, MA 02125

<sup>+</sup> Dept. of Microbiology and Immunobiology, Harvard Medical School, Boston, MA 02115

### Abstract

Point-of-care (POC) diagnostics such as lateral flow and dipstick immunoassays use gold nanoparticle (NP)-antibody conjugates for visual readout. We investigated the effects of NP conjugation, surface chemistries, and antibody immobilization methods on dipstick performance. We compared orientational, covalent conjugation, electrostatic adsorption, and a commercial conjugation kit for dipstick assays to detect dengue virus NS1 protein. Assay performance depended significantly on their conjugate properties. We also tested arrangements of multiple test lines within strips. Results show that orientational, covalent conjugation with PEG shield could improve NS1 detection. These approaches can be used to optimize immunochromatographic detection for a range of biomarkers.

### Keywords

Lateral flow; dipstick; rapid test; dengue; nanoparticle; bioconjugation

### INTRODUCTION

Infectious diseases are constant global health threats due to over-population<sup>1</sup>, poor health care infrastructure, climate change<sup>2</sup>, and increased international travel<sup>3</sup> and shipping<sup>4</sup>.

Dengue virus, a mosquito-transmitted arbovirus, is a risk to over three billion people world-

---

Author Contributions

The manuscript was written through contributions of all authors. All authors have given approval to the final version of the manuscript.

wide<sup>5</sup>. Promising vaccine candidates are currently in development<sup>6, 7</sup>; however, vaccine manufacture and delivery to such a large number of people will be daunting. Rapid diagnostics will continue to play an important role in triaging patients whose primary symptom is fever that could be caused by any one of a number of different pathogens. The availability of inexpensive, rapid, point-of-care (POC) diagnostics will help to direct appropriate care to those who need it most. Paper-based devices are attractive for POCs because they run on capillary forces and thus do not require external power supplies<sup>8</sup>. Furthermore, simple rapid tests do not require sophisticated lab equipment, special storage conditions, or trained personnel, and thus can be used in low-resource and field settings.

In a dipstick sandwich immunoassay, the NP-antibody conjugate is what binds to the biomarker of interest and results in the visible test line color that serves as the ultimate readout to provide the diagnosis. Previous studies have shown that the interface between proteins and NPs can greatly impact not only the structure but also the function of the protein<sup>9, 10</sup>. This is due to surface effects from the protein interacting with the NP surface or surface coating ligand. It is also influenced by how the protein is linked to the NP, where chemical linkages at certain protein sites can result in denaturation. For proteins that are conjugated to NPs by adsorption, where the orientation of the protein is not controlled, configurations that sterically block the binding or active site can inhibit recognition. Often, these interface effects can negatively impact the antigen-binding affinity and specificity.

Reports have shown that capitalizing on the enhanced binding effect from controlled orientation of antibodies can lead to order of magnitude increases in signal compared to random orientation. Parolo et al. showed that by lowering the pH below the isoelectric point of antibodies, the antibodies would become positively charged only on their major plane, which is the orientational plane of the antibody that allows for the highest antibody surface area to be exposed. This major plane is away from the targeting (antigen-binding) portion of the antibody, enabling orientational binding<sup>11</sup>. Then, these positive charges on the antibody would interact with the negative charge of a carboxylated gold NP surface. Lysine groups on the major plane of the antibodies were then linked covalently to the carboxyl groups on the surface of the nanoparticles *via* EDC/sulfoNHS chemistry, which orients the antibody relative to the nanoparticle. Other strategies for orientational binding of antibodies include using protein G to bind to the Fc portion of antibodies<sup>12, 13</sup>. Thus, the ability of the NP-bound antibody to bind to its antigen is subject to orientation-specific surface interactions. However, these reported conjugations typically involve complex processes of forming unique linkers or modifying the surface of the nanoparticle to develop the orientational linkage. Furthermore, many reported orientational conjugations do not verify that they are able to block non-specific effects fully because the assays used to validate the conjugations involve multiple washing and amplification steps, which minimize the effect of non-specific binding of the conjugates themselves. For visually-read dipstick and lateral flow assays with no subsequent washing steps, it is important that non-specific binding be negligible to minimize false positives. These procedural points can have critical ramifications on the ability of a POC assay to be clinically useful. Gold NPs have been used extensively as contrast agents in a variety of micro/paperfluidic tests, and recent reports have shown these tests can be expanded beyond simple formats to fluidic arrays of various designs for multiplexing and lowering the limit of detection<sup>14, 15</sup>. Here, we compared approaches for

conjugating antibodies to gold NPs and characterized the resulting NP-antibody conjugates in detecting a target biomarker in dipstick flow tests. The chosen target was dengue virus NS1 protein, which is secreted into the blood stream and serves as an early marker of dengue viral infections<sup>16</sup>. We find that the nature of the NP-antibody conjugation and the NP surface chemistry significantly improves NP-antibody conjugate binding to NS1, consequently enhancing test line intensity while lowering the limit of detection (LOD). We offer key strategies for optimizing NP-antibody conjugates for detecting biomarkers in immunochromatographic assays.

## EXPERIMENTAL

### Preparation of dengue NS1 monoclonal antibodies and dengue NS1 sample

Dengue anti-NS1 hybridomas were obtained by injecting mice with dengue virus 2 New Guinea C intracranially in the laboratory of Dr. Michael Diamond. The antibodies were produced in the laboratory using routine cell culture methods by expansion and collection of the cell supernatant in ultra low Fetal Calf Serum media, followed by purification of the IgG using Protein L affinity chromatography (HiTrap® Protein L, GE Healthcare) in an automated affinity chromatography protein purification system using manufacturer suggested buffers (Profinia, BioRad). Protein L was used as opposed to Protein G to eliminate bovine IgG from the eluted purified antibody solution. Antibodies were prepared at 1 mg/ml and stored at  $-80^{\circ}\text{C}$  until use. Quality control of the antibodies was monitored using an Agilent Tape Station for protein chromatography. Lateral flow chromatography tests showed that dengue NS1 antibodies 9NS1<sup>17</sup> and DV2-1 formed a functional pair, and were thus used in this study. Supernatants from Vero cells infected with dengue virus serotype 2 and recombinant dengue NS1 serotype 2 produced in 293 human cells (The Native Antigen Company, United Kingdom) were used as a source of NS1 protein for dipstick chromatography experiments.

### Gold NP synthesis

Gold NPs, ~30 nm, were synthesized by reducing chloroauric acid ( $\text{HAuCl}_4$ ) with sodium citrate, as described by Frens<sup>18</sup>. Briefly, 45.5 mL of deionized ultra filtered (DIUF) water was boiled under reflux while stirring with 0.5 ml of 1%  $\text{HAuCl}_4 \cdot 3\text{H}_2\text{O}$  (chloroauric acid trihydrate, Sigma). One mL of 1% sodium citrate ( $\text{HOC}(\text{COONa})(\text{CH}_2\text{COONa})_2 \cdot \text{H}_2\text{O}$ , Mallinckrodt Chemicals) was added and allowed to stir for at least 30 min under boiling reflux.

### NP conjugation

Directional conjugation<sup>19</sup> was achieved by attaching a heterobifunctional linker with a hydrazide on one end and a dithiol on the other, linked by a short polyethylene glycol (PEG) chain (hydrazide dithiolalkane aromatic PEG6-NHNH<sub>2</sub>, Sensopath Technologies). First, the antibody buffer was exchanged to 40 mM HEPES (pH 7.4) by dilution/concentration using a 10 kD centrifuge filter. The final concentration of the antibody was 1 mg/mL. Then, antibodies were exposed to 10 mM final concentration of sodium periodate ( $\text{NaIO}_4$ , Sigma) at a 9:1 antibody to  $\text{NaIO}_4$  volume ratio for 40 min at room temperature, oxidizing the carbohydrate moieties on the Fc region of the antibody to aldehydes. Then, an excess of

linker (2  $\mu\text{L}$  of 3.33 mg/ml in ethanol) was added to the oxidized antibodies for 45 min, leading to linkage between the aldehyde group of the antibodies and the hydrazide on the linker. To remove unreacted linker, antibodies were concentrated in PBS using a 10 kD centrifugal filter column (Amicon) and resuspended in 2% by weight PEG (8kD, Sigma) in PBS at 1 mg/mL.

To conjugate antibodies to the NPs, 2.5  $\mu\text{g}$  of either antibodies + linker (for active conjugation) or antibodies alone (for passive conjugation) were diluted in 40 mM HEPES (pH 7.4–7.8) to a total volume of 500  $\mu\text{L}$  and mixed with 500  $\mu\text{L}$  of as-synthesized ( $\sim 7 \times 10^{10}$  particles/mL) gold NPs for 30 min at room temperature. For PEG backfill, 0.5% w/v 1 X 10<sup>-4</sup> M 5 kD mPEG-SH (Nanocs) was added to the antibody/gold NP solution for 10 min. Following this, for both PEG backfill and no PEG backfill, 10% w/v of 2% PEG (8 kD) in PBS was added, and finally, NP-antibody conjugates were centrifuged at 3000 X g for 30 min and resuspended in 2 % PEG in PBS at 1X10<sup>11</sup>– 1X10<sup>13</sup> particles/mL, depending on type of conjugate. Commercial conjugation was performed using the InnovaCoat <sup>®</sup>GOLD-200D 40 nm Gold Particle Kit from Innova Corporation (Cambridge, United Kingdom) following manufacturer's instructions.

### Characterization of NP conjugates

NP conjugates were characterized using UV Vis, DLS, zeta potential, and transmission electron microscopy (TEM). UV-Vis spectra between 400–800 nm were acquired with a Cary 100 spectrophotometer (Varian). Dynamic light scattering size and zeta potential measurements were taken with disposable cuvettes in a ZetaSizer Nano Series (Malvern). Size distributions were obtained using the Intensities distribution and zeta potential values were obtained using the Smoluchowski analysis method.<sup>20</sup> Each size and zeta measurement was taken at several acquisitions automated by the machine to assess precision in measurements. TEM images of the NPs were taken with an FEI Tecnai Multipurpose TEM (G2 Spirit TWIN) with a 120 kV source.

### Quantification of antibodies per NP

The number of antibodies per NP was quantified by measuring the amount of fluorescently-labeled antibody remaining in solution after the conjugation reaction occurred<sup>21</sup>. For fluorescent labeling, mouse antibodies that were coupled to the fluorophore DyLight ( $\lambda_{\text{ex}} = 654 \text{ nm}$ ,  $\lambda_{\text{em}} = 673 \text{ nm}$ , Thermo Scientific) were conjugated to the gold NPs. Conjugated NPs were centrifuged at 4,000 X g for 30 min, resulting in a dark red pellet with clear supernatant. Unbound antibodies in the supernatant were quantified by fluorescence (Horiba Jobin Yvon), and this value was subtracted from the fluorescence of initial antibody + fluorophore, allowing estimation of the number of antibodies conjugated to the NPs (Supplemental Fig. S2). NP concentration was calculated from its absorbance at the surface plasmon resonance (SPR) and a molar extinction coefficient for 30 nm gold NPs of  $\epsilon = 3.6 \times 10^9 \text{ M}^{-1}\text{cm}^{-1}$ . For commercial NPs,  $\epsilon = 9.3 \times 10^9 \text{ M}^{-1}\text{cm}^{-1}$  (corresponding to 40 nm gold NPs)<sup>22, 23</sup>. Using these values, the number of antibodies per NP was calculated for each conjugation based on an average of 6 measurements for lab-made conjugates, and 3 measurements for commercial conjugates (Supplemental Table 1). A single measurement

was obtained for control gold NPs without conjugation to fluorophore-antibody, and antibody alone.

### Preparation of test strips

Nitrocellulose membrane (Millipore, Capillary flow time 4 cm/240 sec, 1.5 cm wide) was cut by a benchtop laser cutter (Universal Laser Systems VLS2.30, Scottsdale, AZ) equipped with a 10.6  $\mu\text{m}$  CO<sub>2</sub> laser at 25 W, 0.13 mm spot size, at 35 % power and 100 % speed in vector mode to ensure cutting through the membrane and minimal tearing of the edges of strips. Rectangular detection areas cut into each membrane strip were ~2.8 mm wide X 1.8 mm high, with a distance of 3.6 mm between the centers of each detection area. These rectangular areas were cut wider than the rest of the strip to allow the user to easily identify where each test or control band should appear, as well as slow the flow down at the test and control areas. The wick overlapped the membrane by ~16.4 mm to facilitate miniaturization of the device while minimizing potential cross flow between areas. The larger detection areas allow for ease of visualization and maximum interaction time with the sample<sup>24</sup>.

### Printing antibodies

Antibodies were printed on nitrocellulose membrane using an automated Digilab dispenser system (Microsys) with a ceramic tip of pore size 190  $\mu\text{m}$  (Digilab). Antibodies were line-dispensed in 0.05  $\mu\text{L}$  drop volumes at 1  $\mu\text{L}/\text{cm}$  and pitch of 0.5 mm. The test area on a strip was ~2.8 mm wide. For the experiment comparing multiple stripes of immobilized antibody, we printed 2 mg/ml anti-dengue NS1 antibody, 9NS1, multiple times. Active conjugates with PEG backfill were used at a NP-antibody conjugate concentration of 0.06 nM, and NS1 was from supernatants of dengue virus-infected Vero cells.

### Running the Dipstick Assay

Unless otherwise noted, for all tests 0.4  $\mu\text{g}/\text{mm}$  (equivalent to 0.66  $\mu\text{L}$  of anti-NS1 antibody 9NS1 at 2 mg/mL) was printed onto the nitrocellulose test area. Test samples were either purified recombinant NS1 from dengue serotype 2 produced in 293 human cells, or supernatants of monkey kidney cell cultures (Vero) infected with patient-isolated dengue virus serotype 2 at low clinical passage number. The Vero cells secrete dengue NS1 protein during dengue virus infection.

Controls of only human serum were run for each conjugate concentration. The control line in all tests was an anti-Fc antibody that binds with antibody-conjugated NPs.

The dipstick assay consisted of a nitrocellulose strip onto which antibodies for the antigen NS1 from dengue virus serotype 2 (9NS1) were printed at the test area, and antibodies that recognized the Fc region of the antibody from NP-antibody conjugates were printed at the positive control area (Fig. 1b). The nitrocellulose membrane had four detection areas (each area ~2.8 X 1.8 mm<sup>2</sup>) where the top two areas were used for test and control areas and the bottom two were used to define background in image analysis (Supplemental Fig. S1).

Buffer solution, sample, and NP-antibody conjugate solution were mixed in a 1.7 mL eppendorf tube. Buffer solution was comprised of 1:2:2 volume ratio of 50% w/v sucrose in

water: 1% v/v Tween 80 in PBS : 2% w/v 8kD PEG in PBS, total buffer solution volume of 20  $\mu$ L. Sample volumes of 40  $\mu$ L (of various concentrations of purified dengue NS1 protein (Native Antigen) or dilutions of supernatant of dengue-infected Vero cells) were then added to the buffer mixture, bringing the volume to 60  $\mu$ L. Unless otherwise noted, gold NP-antibody conjugate solutions were added to the tube at a final concentration of 0.06 nM (2 X 10<sup>9</sup> particles in 60  $\mu$ L). The amount of NP-antibody conjugate added to each tube was 0.5–1  $\mu$ L of ~5 nM gold NP-antibody, depending on the concentration of the pelleted conjugate solution, to achieve 2 X 10<sup>9</sup> NPs per tube. A laser-cut nitrocellulose membrane (Millipore, Capillary flow time 4 cm/240 sec, 1.5 cm wide, Methods) that was printed with antibodies was attached to an absorbent pad (VWR blotting paper) *via* a one-sided adhesive backing (Lohmann). Before the membrane was assembled into a full test strip with the absorbent pad, the membrane printed with antibodies was allowed to fully dry (by visual inspection) at room temperature (45 min) to ensure printed antibodies did not prematurely wick up the membrane. The membrane was then placed on an adhesive (~ 5 X 10 mm<sup>2</sup>), followed by the absorbent pad (~5 X 30 mm<sup>2</sup>). The absorbent pad overlapped the top of the membrane by ~2 mm ensuring contact. The nitrocellulose membrane was placed vertically with the absorbent pad at the top in the eppendorf tube containing buffer, sample, and NP-antibody conjugate. The test was run until all solution reached the absorbent pad. Positive test bands were often visible within ~5–10 min, and test runs were allowed to run for 3–4 h to reach completion. Presence of antigen could be detected by dark colored bands at both the test and positive control areas due to the presence of NPs. When NS1 was present, a colored test band appeared; when NS1 was absent, no test band appeared. The positive control band indicated that flow occurred and that the test was valid.

### Quantification of signal intensities

Strips were imaged using a lightbox (SysGene) with the same exposure settings for all strips (80 ms exposure time). ImageJ<sup>25</sup> was used to quantify intensity of each test and background area on the strip (Supplemental Fig. S1). All background-subtracted intensities were normalized to a calibration strip intensity and kept constant between each image. The calibration strip was a test strip with dark bands drawn with a black marker on both control and test areas, to simulate the darkest signal achievable with our test. Before analysis, images were converted to 8-bit grayscale to create a single intensity value for each pixel. 8-bit images were inverted to quantify test bands in a way that gave a higher intensity for darker pixels. Regions of interest (ROIs) 0.3  $\times$  0.06 pixels sq. were used for test and background areas for all strips. Each ROI's average gray value was measured and normalized by the calibrating strip's ROI, and plotted against dengue NS1 antigen concentration to gain titration curves. Each strip was run in triplicate and an average intensity was plotted for each detection area. Additional details are in Supplemental Fig. S1.

### Limit of Detection Calculations

Assay limit of detection (LOD) was calculated by fitting band intensities to a sigmoidal (Supplemental Equation 1) to the average of experimental test area intensity values at 0, 5, 25, 75, 200, and 500 ng/ml using the Matlab curve fitting toolbox. LOD was defined as the minimum concentration that yielded an average test area intensity that was exceeded by 3 times the standard deviation of a blank (sample without antigen) over the average intensity

of the blank<sup>26</sup>. Molarity of LOD was determined using a molecular weight of 50 kD for Dengue NS1<sup>27</sup>.

## RESULTS

### Properties of the NPs and NP-antibody conjugates

Gold NPs have been used in a variety of biomedical sensing applications because of their tunable optical properties, ease of surface functionalization, biocompatibility, and size<sup>28–33</sup>. To detect an antigen of interest, NPs are conjugated to antibodies that recognize the antigens, and the strong optical absorption of NPs enables colorimetric detection by eye. Here, we compared three conjugation strategies (Fig. 1a): i) directional, covalent conjugation *via* dithiol linker between the gold NP surface and the non-targeting, (Fc) region of the antibodies<sup>19</sup>, called active conjugation, ii) passive adsorption of antibodies to the NP surface, or passive conjugation and iii) a commercial covalent conjugation kit (Innova Biosciences©), called commercial conjugation here.

Citrate-capped gold NPs were synthesized as previously described<sup>18</sup>. NPs were attached to the antibodies either covalently or passively (Methods). Commercial NPs were covalently conjugated to antibodies using the manufacturer's recommended protocol. The commercial NPs use a covalent attachment chemistry that links to proteins *via* lysine residues, although details of the NP surface chemistry and buffer conditions were not specified by the manufacturer. Transmission electron microscopy (TEM) images of NP-antibody conjugates showed similar morphologies, yielding roughly spherical particles with  $\langle D \rangle \sim 32$  nm for lab-made citrate-capped NPs, and  $\langle D \rangle \sim 38$  nm for commercial gold NPs (Fig. 2a, Supplemental Information Table 2).

Dynamic Light Scattering (DLS) measured the hydrodynamic diameter ( $D_H$ ) of the samples to determine if antibodies had attached to the NP surface *via* a monolayer or multilayer, and if aggregation occurred (Fig. 2b and Supplemental Information Table 2).  $D_H$  of NPs increased by  $\sim 25$  nm upon antibody conjugation. With both antibody conjugation and PEG backfill,  $D_H$  increased by  $\sim 45$  nm for active conjugation and  $\sim 65$  nm for passive conjugation. Interestingly, the commercial NPs did not change in  $D_H$  after antibody conjugation. This could potentially be due to the proprietary NP surface coating, which may be displaced by antibodies upon conjugation. To determine colloidal stability of the conjugates, we measured their absorbance spectra. Citrate-capped NPs and NP-antibody conjugates had narrow SPR peaks, confirming the NPs and conjugates were stable and not aggregated (Fig. 2c).

Zeta potential measurements showed that all NP-antibody conjugates were negatively charged (Fig. 2d and Supplemental Information Table 2). Citrate-capped gold NPs had a zeta potential of  $-37$  mV which increased to  $-28$  and  $-27$  mV for active and passive conjugation, respectively. After PEG backfill, the zeta potential further increased to  $-21$  and  $-16$  mV for active and passive conjugation, respectively. Zeta potential of commercial conjugates ( $-20$  mV) was comparable to lab-made conjugates after PEG backfill. These results confirm successful NP conjugation to the antibodies and that the conjugates were stable in solution.

Antibody coverage on the NPs was measured. NP concentration was determined from absorbance spectra and their molar extinction coefficients<sup>22, 23</sup> (Methods; Supplemental Information Fig. S2). Lab-made conjugates yielded an average 60–65 antibodies per NP (no significant difference among all lab-made conjugates,  $p = 0.44$  using one-way ANOVA). Commercial conjugation was found to have a significantly lower coverage of ~10 antibodies per NP, 6–7 X lower than lab-made commercial particles (Fig. 3a, Supplemental Table 1).

### Effect of NP-antibody conjugation strategy on assay performance

NPs conjugated to anti-dengue NS1 antibody DV2–1 were tested in dipstick assays (Fig. 1b). We compared the ability of the different NP-antibody conjugates to detect NS1 in assays in two ways: (1) at the same NP concentration and (2) at the same antibody concentration in the conjugate.

Mouse anti-dengue NS1 monoclonal antibody, DV2–1, was conjugated to the NP, and mouse anti-dengue NS1 monoclonal antibody, 9NS1, was immobilized on the strip by printing (Methods). Antibodies that recognized the Fc region of the antibody on the conjugates were printed at the positive control area (Fig. 1b). The bottom two areas were left blank and used to define background in image analysis (Methods). Strips were placed vertically in a solution with NS1 and NP-antibody conjugates in human serum and the fluid wicked through (Methods).

Test line intensities for each of the conjugates increased with increasing NS1 concentration (Fig. 4a). For no NS1, the test line areas showed no band. For all strips, the control lines (upper) showed bands, confirming that the NP-antibody conjugates flowed through the test strip.

To quantitatively compare the performance of the different conjugates, we calculated their LODs (Fig. 4b, left). Test line intensities were fit to a sigmoidal and LOD was determined as the minimum concentration that yielded an average test area intensity 3 times the standard deviation of a blank (sample without antigen) over the average intensity of the blank (Methods, Limit of Detection Calculations, Supplemental Equation 1)<sup>26</sup>. Sigmoidal fits yielded  $R^2 = 0.9990$  for active conjugation, 0.9997 for passive conjugation, and 0.9930 for commercial conjugation. The calculated LOD for active NP-antibody conjugates was 13 ng/ml ( $2.6 \times 10^{-10}$  M), for passive 34 ng/mL ( $6.8 \times 10^{-10}$  M), and for commercial 65 ng/mL ( $1.3 \times 10^{-9}$  M) (Fig. 4b, right). Thus, lab-made NPs with active conjugation yielded a LOD 5X lower than commercial NPs. Similar LOD trends were observed for all types of conjugates using supernatants of infected Vero cells as the sample (Supplemental Information, Fig. S3). These results suggest that lab-made active conjugates yield improved binding affinity and LOD performance especially for NS1 concentrations in range of 25–250 ng/mL.

Next, the assay was performed for solutions with the same amounts of DV2–1 antibodies (Fig. 3). Because antibody coverage on the commercial NPs was much lower, (Fig. 3a, Supplemental Table 1), the NP concentration in the solution for the dipstick assay had to be 6–7X higher to obtain the same antibody concentration as the lab-made NP-antibody conjugates. Thus, lab-made NP-antibody conjugate concentrations ranged from  $8 \times 10^{-3}$  – 9

$10^{-3}$  nM, while the commercial conjugate concentration was  $5.4 \times 10^{-2}$  nM (Supplemental Table 3). Commercial conjugates had 2.3X significantly higher test band intensities than both the active and passive conjugates (Fig. 3c,  $p < 0.05$ , one way ANOVA for all conjugates, while  $p = 0.44$  one way ANOVA for only lab-made conjugates). This could be explained by the fact that the commercial conjugates were at a higher NP concentration relative to lab-made conjugates, even though the calculated numbers of NP-bound antibodies were equivalent. Thus, when normalized by the number of antibodies conjugated to the NPs, the commercial conjugates led to a higher intensity test band compared to lab-made conjugates. Human serum controls for these strips showed negligible signal (Supplemental Fig. S4a,b).

### Effect of NP surface chemistry

We investigated how modification of NP surface chemistry by PEG backfilling affected test strip performance. Active conjugation samples were subjected to a subsequent functionalization step of additional methoxy-polyethyleneglycol-thiol (mPEG-SH, 5 kD), which is commonly used to passivate bare NP surfaces and decrease non-specific adsorption<sup>34–36</sup>. mPEG-SH was chosen instead of bovine serum albumin (BSA) for passivation because of the covalent attachment of the mPEG-SH to the NP and the ability of PEG to impart stealth properties in physiologically relevant media. We compared active conjugation of the NP-antibody conjugates with and without PEG backfill for fixed conjugate concentration and printed antibody (Fig. 5a).

Test band intensity titration curves (Fig. 5b) showed that PEG backfilled samples (red circles) had a slightly sharper slope compared to no PEG backfill (blue squares). This showed that PEG backfilling has a small but measurable effect on test line intensity, and acts to increase the binding affinity of the conjugate for NS1. This shows that surface treatment can improve test performance presumably from decreased non-specific protein interactions<sup>34–36</sup>.

### Optimizing the amounts of NP conjugates and printed antibody

For further optimization, we varied amounts of conjugate and immobilized antibody to probe test line intensity dependence on concentration of reagent. The amount of striped antibody on the nitrocellulose ( $0.4 \mu\text{g}/\text{mm}$ , or  $0.66 \mu\text{L}$  of anti-NS1 antibody 9NS1 at  $2 \text{ mg}/\text{mL}$ ) and NS1 concentration were fixed, and NP-antibody conjugate concentration was varied in the range  $0\text{--}0.11 \text{ nM}$  (Fig. 3d). Test line intensity increased with concentration and plateaued at  $0.06 \text{ nM}$ . Control test strips run only with human serum showed negligible test signal (Supplemental Fig. S4a,c).

We also investigated the effect of the concentration of the immobilized 9NS1 antibody by varying the number of prints onto the same test area. Increasing print number to 2 increased test line intensity significantly (Fig. 6a, lane 1 vs. lane 2; Fig. 6b,  $p < 0.05$  two-tailed t test between  $0.2$  and  $0.4 \mu\text{g}/\text{mm}$ ). However, the signal intensity saturated at beyond 2 prints (Fig. 6b;  $p = 0.3$  one way ANOVA between test band intensity for  $0.4\text{--}1 \mu\text{g}/\text{mm}$ , or stripes 2–5X).

## In-line multiplexing

Multiplexed assays that can test for multiple biomarkers simultaneously are attractive for differential diagnosis in the field. This can be achieved by creating branched strip structures where each branch tests for a different biomarker. However, this strategy requires more sample volume in order to have enough for each of the different branches<sup>37-39</sup>, which could be an issue for limited sample amounts. Printing different capture antibodies in different locations on a single lane is potentially an economical way to provide in-line multiplexing. However, as the NP-antibody-antigen migrates along the strip, its concentration may be depleted. We investigated the effect of printing multiple stripes of 9NS1 in different locations on the test line intensity (Fig. 7). For two test areas (strip 1), the lower area was darker than the upper one, showing that the first area the sample encounters consumes the NP-antibody-NS1 so that there is less to bind to subsequent areas. Control strips (strips 2, 3) showed that the intensity is not simply due to where the line is positioned. Increasing the concentration of the Abs printed on the nitrocellulose can counter the effect of conjugate-NS1 consumption at each test line. Multiple prints at the upper test area (2X and 3X) determined that tripling the print number could make the intensity of the upper line match the lower area (strips 4, 5). This differential effect could not, however, be countered simply by increasing conjugate concentration (2X and 3X), as the bottom test area remained darker than the top (strips 6, 7). These results show that consumption of sample for in-line multiplexing can impact test line intensity, but multiple prints can mitigate it.

## DISCUSSION

Rapid point-of-care diagnostics hold tremendous potential for detecting biomarkers at low cost for use in austere environments. However, the overall performance of the device depends on the antibody affinities, the NP conjugation/coupling efficiencies, non-specific background signal, and flow rates. NP conjugation and surface modification chemistries can influence the sensitivity of dipstick and lateral flow immunoassays. Studies of NP-protein conjugates have shown that conjugation strategy affects protein structure, orientation, and consequently protein function and ability to bind to targets<sup>9, 10</sup>. In addition, how the antibody on the test line is immobilized can also influence binding. By testing different NP preparations, antibody coupling strategies, and antibody depositions, we show that changing these parameters can improve LOD for dengue virus NS1 protein.

### Comparing lab-made to commercial particles

In general, lab-made particles are significantly less expensive to prepare than commercially available NPs, but are somewhat less convenient because of preparation time. Comparing band intensities in the dipstick test as a function of fixed NP concentration, we found that the lowest LODs were achieved for lab-made NPs and active (covalent, directional) antibody conjugation (Fig. 4). At NS1 concentrations 200 ng/mL, all of the NP conjugates performed equivalently. However, test lines were visible by eye at 25 and 75 ng/ml with the active conjugation onto lab-made particles, but not the commercial particles.

Correspondingly, active and passive conjugation on lab-made particles yielded lower calculated LODs of 13 and 34 ng/mL ( $2.6 \times 10^{-10}$  M and  $6.8 \times 10^{-10}$  M), respectively, compared to commercial conjugation, which had an LOD of 65 ng/mL ( $1.3 \times 10^{-9}$  M) for a

given conjugate concentration. Thus, active conjugation yielded a calculated, interpolated LOD that was 5X lower than commercial conjugation. While both active and passive methods conjugated approximately the same number of antibodies per NP, the commercial particles had a 6–7X lower antibody density (Fig. 3a). Because of the proprietary nature of the commercial particles, the cause for the lower antibody surface density compared to the lab-made NPs is not known but could be related to surface stabilizers or passivants that reduce antibody reactivity at the NP surface, or the possibility that the number of available reactive groups is smaller on the commercial particles than on the lab-made NPs.

Active and passive conjugation to lab-made NPs had similar antibody densities (Fig. 3a). Because active conjugation resulted in a lower LOD than passive conjugation, test performance is improved by covalent, orientational conjugation using a directional linker. Antibodies passively adsorbed to NPs can assume a variety of configurations on the NP surface that are sterically hindered from binding to the NS1, thereby increasing the LOD. If the NP-antibody conjugates were compared for a constant amount of antibody on the surface of the NPs, then commercial conjugates had the highest intensity at the test area due to the fact that they have low coverage, and thus higher NP concentration than lab-made NPs. The higher NP concentration led to a higher test line intensity at a given NS1 concentration (Fig. 3b). This suggests that one strategy for increasing signal intensity is to lower antibody coverage and increase the NP-antibody conjugate concentration. Here we prepared the conjugates using optimized protocols from previous reports and manufacturer's protocols, but further characterization (e.g. varying antibody:NP ratios for each type of conjugate) would further elucidate the conjugates' binding capabilities.

These results suggest that, at constant NP concentration, lab-made active conjugates yield improved binding and LOD performance that was especially notable for NS1 concentrations in the range of 25– 250 ng/mL, in the stages of very early detection. However, at saturation (>500 ng/mL) the performance of the various conjugates was similar.

### Surface chemistry

Changing the surface chemistry of NP-antibody conjugates can improve their ability to bind to the NS1 and result in higher test line intensities. While the effect may appear slight, it does increase the net binding affinity for the NS1 target. Benefits of PEG backfilling have been observed previously for proteins and DNA on NP surfaces, and attributed to reduction of non-specific adsorption<sup>34–36</sup>. While not observed here, excessive PEG backfilling can reduce target binding due to steric hindrance, particularly when the binding moiety is small relative to PEG chain length<sup>40</sup>. The comparison enables evaluation of the impact of PEG backfilling on the binding affinity of the immobilized antibody for its target.

### Immobilized antibody

We also determined that the intensity of the test band is dependent on both conjugate and printed antibody concentration up to a saturation point (Figs. 3c and 6). While printing once at a higher antibody concentration could potentially achieve the same signal increase, we found that higher antibody concentrations (>2 mg/mL) did not flow well out of the printing tip (results not shown). For multiple test lines of the same antibody, the first test line that a

sample fluid encounters is much darker than subsequent test lines due to consumption of the NP-antibody-NS1 complex from the sample as it passes over the immobilized antibody. These are considerations that should be taken into account for in-line multiplexed tests.

### Relevant concentration ranges

Based on the titration curves, improvements to the NP-antibody conjugates will not affect detection when the NS1 is high, as all test line intensities are high and have similar values. However, the NS1 concentration in the plasma and most likely other biological fluids varies depending on how many days post infection when the patient is assayed. NS1 concentrations are low at early times post-infection (~1 day), and it is during this period where modifications to the NP-antibody conjugates can be important. Furthermore, for other infectious diseases, the concentration of the antigen of interest may be very low in patient blood, or the natural affinity of the available antibody for the antigen may be low. It is for these cases that the properties of the conjugates and immobilized antibodies can be leveraged to improve LOD and performance. Thus, knowing the concentration dependence gives one the opportunity to improve the molecular properties of the NP-antibody conjugate to increase test line intensities. Unfortunately, for emerging infectious diseases, the concentration ranges of the antigen are often not known beforehand due to limited availability of patient samples, so strategies for improving LODs for different concentration ranges are critical. It may be the case that the amounts of NPs and striped antibody may need to be empirically determined to get the best signal, perhaps for each target concentration and NP preparation.

## CONCLUSION

Rapid diagnostics are used in varying settings to detect ligands present at high and low concentrations. Therefore, the reagents and NP surface properties must be tuned to detect ligands under conditions of their use. Conjugation strategy, surface chemistry of conjugates, and concentration of printed antibody and conjugates can all be optimized to yield POC devices that can have low limits of detection. This work describes approaches that can be used in developing effective, low cost diagnostic devices. Our data suggest that developing NP-antibody conjugates in-house could be more cost effective than purchasing commercial conjugation kits, and can lead to a lower LOD. It also underscores the fact that the NP-antibody properties influence the sensitivity of the device. We estimate that developing conjugates in-house decreases cost by 70% compared to commercial kits (Supplemental Table 4). The cost of a test strip is due mostly to the antibodies, so lowering antibody coverage on the NP and using a higher NP-antibody conjugate concentration (up to a saturation point) can decrease cost while also increasing test line intensity. These are factors that have implications for development of a device for use outside of the typical lab, in the field.

## Supplementary Material

Refer to Web version on PubMed Central for supplementary material.

## REFERENCES

1. Wen TH; Lin MH; Teng HJ; Chang NT, Incorporating the human-Aedes mosquito interactions into measuring the spatial risk of urban dengue fever. *Applied Geography* 2015, 62, 256–266.
2. Naish S; Dale P; Mackenzie JS; McBride J; Mengersen K; Tong S, Climate change and dengue: a critical and systematic review of quantitative modelling approaches. *Bmc Infectious Diseases* 2014, 14. [PubMed: 24405719]
3. Zhou YR; Coleman WD, Accelerated Contagion and Response: Understanding the Relationships among Globalization, Time, and Disease. *Globalizations* 2016, 13 (3), 285–299.
4. Tatem AJ, Mapping population and pathogen movements. *International Health* 2014, 6 (1), 5–11. [PubMed: 24480992]
5. Bhatt S; Gething PW; Brady OJ; Messina JP; Farlow AW; Moyes CL; Drake JM; Brownstein JS; Hoen AG; Sankoh O; Myers MF; George DB; Jaenisch T; Wint GRW; Simmons CP; Scott TW; Farrar JJ; Hay SI; Inst M, The Global Distribution and Burden of Dengue. *Influence of Global Environmental Change on Infectious Disease Dynamics: Workshop Summary 2014*, 297–310.
6. George S; Wong M; Dube T; Boroughs K; Stovall J; Luy B; Haller A; Osorio J; Eggemeyer L; Irby-Moore S; Frey S; Huang C; Stinchcomb D, Safety and Immunogenicity of a Live Attenuated Tetravalent Dengue Vaccine Candidate in Flavivirus-Naive Adults: A Randomized, Double-Blinded Phase 1 Clinical Trial. *The Journal of Infectious Diseases* 2015, 212 (7), 1032–1041. [PubMed: 25791116]
7. Kirkpatrick BD; Durbin AP; Pierce KK; Carmolli MP; Tibery CM; Grier PL; Hynes N; Diehl SA; Elwood D; Jarvis AP; Sabundayo BP; Lyon CE; Larsson CJ; Jo M; Lovchik JM; Luke CJ; Walsh MC; Fraser EA; Subbarao K; Whitehead SS, Robust and Balanced Immune Responses to All 4 Dengue Virus Serotypes Following Administration of a Single Dose of a Live Attenuated Tetravalent Dengue Vaccine to Healthy, Flavivirus-Naive Adults. *The Journal of infectious diseases* 2015, 212 (5), 702–10. [PubMed: 25801652]
8. Martinez AW; Phillips ST; Whitesides GM; Carrilho E, Diagnostics for the developing world: microfluidic paper-based analytical devices. *Anal Chem* 2010, 82 (1), 3–10. [PubMed: 20000334]
9. Ahmed V; Kumar J; Kumar M; Chauhan MB; Dahiya P; Chauhan NS, Functionalised iron nanoparticle-penicillin G conjugates: a novel strategy to combat the rapid emergence of b-lactamase resistance among infectious micro-organism. *Journal of Experimental Nanoscience* 2015, 10 (9), 718–728.
10. Galbiati E; Cassani M; Verderio P; Martegani E; Colombo M; Tortora P; Mazzucchelli S; Proserpi D, Peptide-nanoparticle ligation mediated by cutinase fusion for the development of cancer cell-targeted nanoconjugates. *Bioconjugate chemistry* 2015, 26 (4), 680–9. [PubMed: 25741889]
11. Parolo C; de la Escosura-Muniz A; Polo E; Grazu V; de la Fuente JM; Merkoci A, Design, Preparation, and Evaluation of a Fixed-Orientation Antibody/Gold-Nanoparticle Conjugate as an Immunosensing Label. *Acs Applied Materials & Interfaces* 2013, 5 (21), 10753–10759. [PubMed: 24095174]
12. Lee IH; Lee JM; Jung Y, Controlled Protein Embedment onto Au/Ag Core-Shell Nanoparticles for Immuno-Labeling of Nanosilver Surface. *Acs Applied Materials & Interfaces* 2014, 6 (10), 7659–7664. [PubMed: 24801432]
13. Kato K; Lian LY; Barsukov IL; Derrick JP; Kim HH; Tanaka R; Yoshino A; Shiraishi M; Shimada I; Arata Y; Roberts GCK, MODEL FOR THE COMPLEX BETWEEN PROTEIN-G AND AN ANTIBODY FC FRAGMENT IN SOLUTION. *Structure* 1995, 3 (1), 79–85. [PubMed: 7743134]
14. Abbas A; Brimer A; Slocik JM; Tian LM; Naik RR; Singamaneni S, Multifunctional Analytical Platform on a Paper Strip: Separation, Preconcentration, and Subattomolar Detection. *Analytical Chemistry* 2013, 85 (8), 3977–3983. [PubMed: 23425068]
15. He J; Boegli M; Bruzas I; Lum W; Sagle L, Patterned Plasmonic Nanoparticle Arrays for Microfluidic and Multiplexed Biological Assays. *Analytical Chemistry* 2015, 87 (22), 11407–11414. [PubMed: 26494412]
16. Amorim JH; Alves RP; Boscardin SB; Ferreira LC, The dengue virus non-structural 1 protein: risks and benefits. *Virus Res* 2014, 181, 53–60. [PubMed: 24434336]

17. Chung KM; Nybakken GE; Thompson BS; Engle MJ; Marri A; Fremont DH; Diamond MS, Antibodies against West Nile Virus nonstructural protein NS1 prevent lethal infection through Fc gamma receptor-dependent and -independent mechanisms. *J Virol* 2006, 80 (3), 1340–51. [PubMed: 16415011]
18. Frens G, Controlled Nucleation for the Regulation of the Particle Size in Monodisperse Gold Suspensions. *Nature Physical Science*: January 1973; Vol. 241, pp 20–22.
19. Kumar S; Aaron J; Sokolov K, Directional conjugation of antibodies to nanoparticles for synthesis of multiplexed optical contrast agents with both delivery and targeting moieties. *Nat Protoc* 2008, 3 (2), 314–20. [PubMed: 18274533]
20. Hunter RJ, *Zeta Potential in Colloid Science: Principles and Applications*. Academic Press Limited: London, 1981.
21. Ciaurriz P; Bravo E; Hamad-Schifferli K, Effect of architecture on the activity of glucose oxidase/horseradish peroxidase/carbon nanoparticle conjugates. *Journal of Colloid and Interface Science* 2014, 414, 73–81. [PubMed: 24231087]
22. Haiss W; Thanh NT; Aveyard J; Fernig DG, Determination of size and concentration of gold nanoparticles from UV-vis spectra. *Anal Chem* 2007, 79 (11), 4215–21. [PubMed: 17458937]
23. Liu X; Atwater M; Wang J; Huo Q, Extinction coefficient of gold nanoparticles with different sizes and different capping ligands. *Colloids and Surfaces B-Biointerfaces* 2007, 58 (1), 3–7.
24. Parolo C; Medina-Sánchez M; de la Escosura-Muñiz A; Merkoçi A, Simple paper architecture modifications lead to enhanced sensitivity in nanoparticle based lateral flow immunoassays. *Lab Chip* 2013, 13 (3), 386–90. [PubMed: 23223959]
25. Abramoff MD MP, Ram SJ, *Image Processing with ImageJ*. *Biophotonics International* 2004, 11, 36–42.
26. Badu-Tawiah AK; Lathwal S; Kaastrup K; Al-Sayah M; Christodouleas DC; Smith BS; Whitesides GM; Sikes HD, Polymerization-based signal amplification for paper-based immunoassays. *Lab on a Chip* 2015, 15 (3), 655–659. [PubMed: 25427131]
27. Libraty DH; Young PR; Pickering D; Endy TP; Kalayanarooj S; Green S; Vaughn DW; Nisalak A; Ennis FA; Rothman AL, High circulating levels of the dengue virus nonstructural protein NS1 early in dengue illness correlate with the development of dengue hemorrhagic fever. *Journal of Infectious Diseases* 2002, 186 (8), 1165–1168. [PubMed: 12355369]
28. Aaron J; Nitin N; Travis K; Kumar S; Collier T; Park SY; José-Yacamán M; Coghlan L; Follen M; Richards-Kortum R; Sokolov K, Plasmon resonance coupling of metal nanoparticles for molecular imaging of carcinogenesis in vivo. *J Biomed Opt* 2007, 12 (3), 034007. [PubMed: 17614715]
29. Huang X; Jain PK; El-Sayed IH; El-Sayed MA, Gold nanoparticles: interesting optical properties and recent applications in cancer diagnostics and therapy. *Nanomedicine (Lond)* 2007, 2 (5), 681–93. [PubMed: 17976030]
30. Mallidi S; Larson T; Tam J; Joshi PP; Karpouk A; Sokolov K; Emelianov S, Multiwavelength photoacoustic imaging and plasmon resonance coupling of gold nanoparticles for selective detection of cancer. *Nano Lett* 2009, 9 (8), 2825–31. [PubMed: 19572747]
31. Sokolov K; Follen M; Aaron J; Pavlova I; Malpica A; Lotan R; Richards-Kortum R, Real-time vital optical imaging of precancer using anti-epidermal growth factor receptor antibodies conjugated to gold nanoparticles. *Cancer Res* 2003, 63 (9), 1999–2004. [PubMed: 12727808]
32. Tallury P; Malhotra A; Byrne LM; Santra S, Nanobioimaging and sensing of infectious diseases. *Adv Drug Deliv Rev* 2010, 62 (4–5), 424–37. [PubMed: 19931579]
33. Zhao LL; Blackburn J; Brosseau CL, Quantitative Detection of Uric Acid by Electrochemical-Surface Enhanced Raman Spectroscopy Using a Multi layered Au/Ag Substrate. *Analytical Chemistry* 2015, 87 (1), 441–447. [PubMed: 25483146]
34. Aubin-Tam ME; Hamad-Schifferli K, Gold nanoparticle cytochrome c complexes: The effect of nanoparticle ligand charge on protein structure. *Langmuir* 2005, 21 (26), 12080–12084. [PubMed: 16342975]
35. Park S; Hamad-Schifferli K, Enhancement of In Vitro Translation by Gold Nanoparticle-DNA Conjugates. *Acs Nano* 2010, 4 (5), 2555–2560. [PubMed: 20384314]

36. Tobio M; Sanchez A; Vila A; Soriano I; Evora C; Vila-Jato JL; Alonso MJ, The role of PEG on the stability in digestive fluids and in vivo fate of PEG-PLA nanoparticles following oral administration. *Colloids and Surfaces B-Biointerfaces* 2000, 18 (3–4), 315–323.
37. Li CZ; Vandenberg K; Prabhulkar S; Zhu XN; Schneper L; Methee K; Rosser CJ; Almeida E, Paper based point-of-care testing disc for multiplex whole cell bacteria analysis. *Biosensors & Bioelectronics* 2011, 26 (11), 4342–4348. [PubMed: 21592765]
38. Lutz BR; Trinh P; Ball C; Fu E; Yager P, Two-dimensional paper networks: programmable fluidic disconnects for multi-step processes in shaped paper. *Lab on a Chip* 2011, 11 (24), 4274–4278. [PubMed: 22037591]
39. Yen C-W; de Puig H; Tam JO; Gomez-Marquez J; Bosch I; Hamad-Schifferli K; Gehrke L, Multicolored silver nanoparticles for multiplexed disease diagnostics: distinguishing dengue, yellow fever, and Ebola viruses. *Lab on a Chip* 2015, 15 (7), 1638–1641. [PubMed: 25672590]
40. de Puig H; Federici S; Baxamusa SH; Bergese P; Hamad-Schifferli K, Quantifying the Nanomachinery of the Nanoparticle-Biomolecule Interface. *Small* 2011, 7 (17), 2477–2484. [PubMed: 21692181]

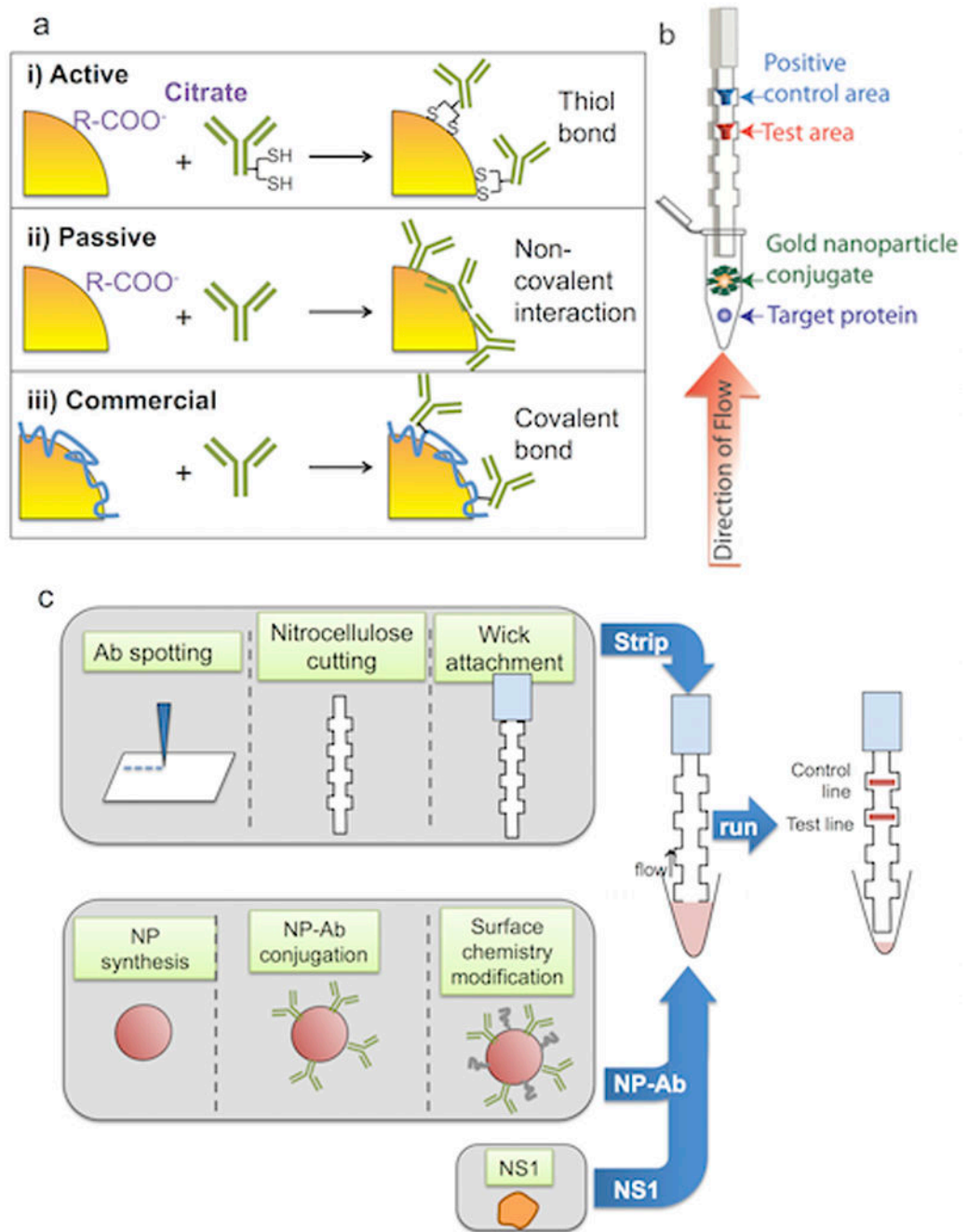


**Figure 1.** Conjugates investigated. (a) Schematic of NP-antibody conjugation strategies i) Active, ii) Passive, and iii) Commercial conjugations. (b) The dipstick assay consisted of a nitrocellulose membrane with a test area for capturing target protein, and a positive control area for gold NP conjugates. (c) schematic showing work flow of dipstick assembly and running of the strip.

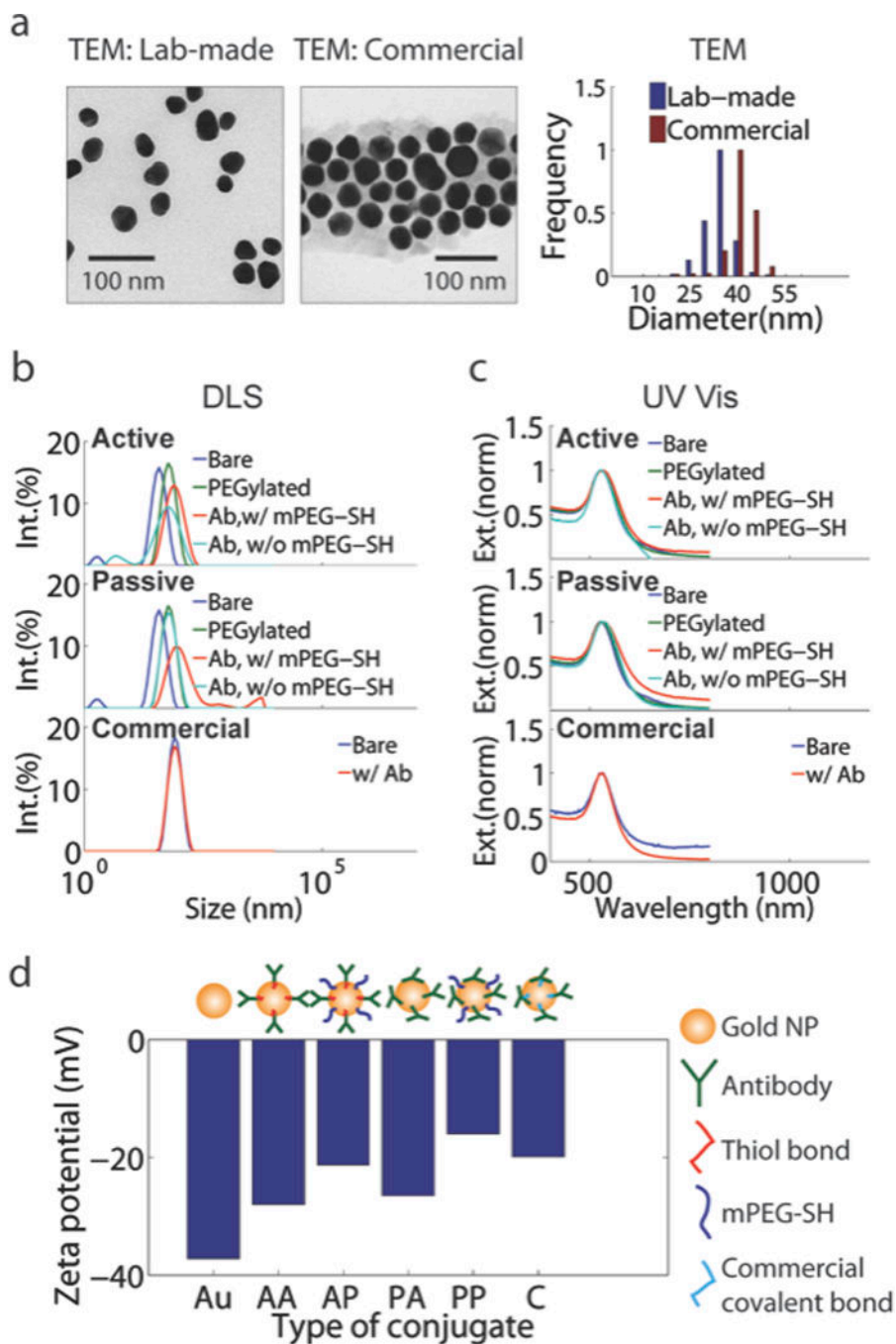


**Figure 2.** Characterization of NP-antibody conjugates. (a) Transmission electron microscope (TEM) images of lab-made actively conjugated NP-antibody conjugates (left) and commercially conjugated NP-antibody conjugates (middle). Scale bars = 100 nm. (Right) Size distribution of lab-made particles  $\langle D \rangle = 31.6 \pm 4.2$  nm ( $n = 373$ ), and commercial particles  $\langle D \rangle = 38.3 \pm 4.2$  nm ( $n = 724$ ). (b) Dynamic light scattering (DLS) for active (top), passive (middle), and commercial (bottom) conjugates. (c) Absorbance spectra of conjugates: active (top), passive (middle), with and without backfill of mPEG-SH, and commercial (bottom) (d) Zeta

potential of conjugates. AA = active antibody conjugation, no mPEG-SH backfill. AP = active antibody conjugation, with mPEG-SH backfill. PA = passive antibody conjugation, no mPEG-SH backfill. PP = passive antibody conjugation with mPEG-SH backfill. C = Commercial nanoparticle-antibody conjugation.

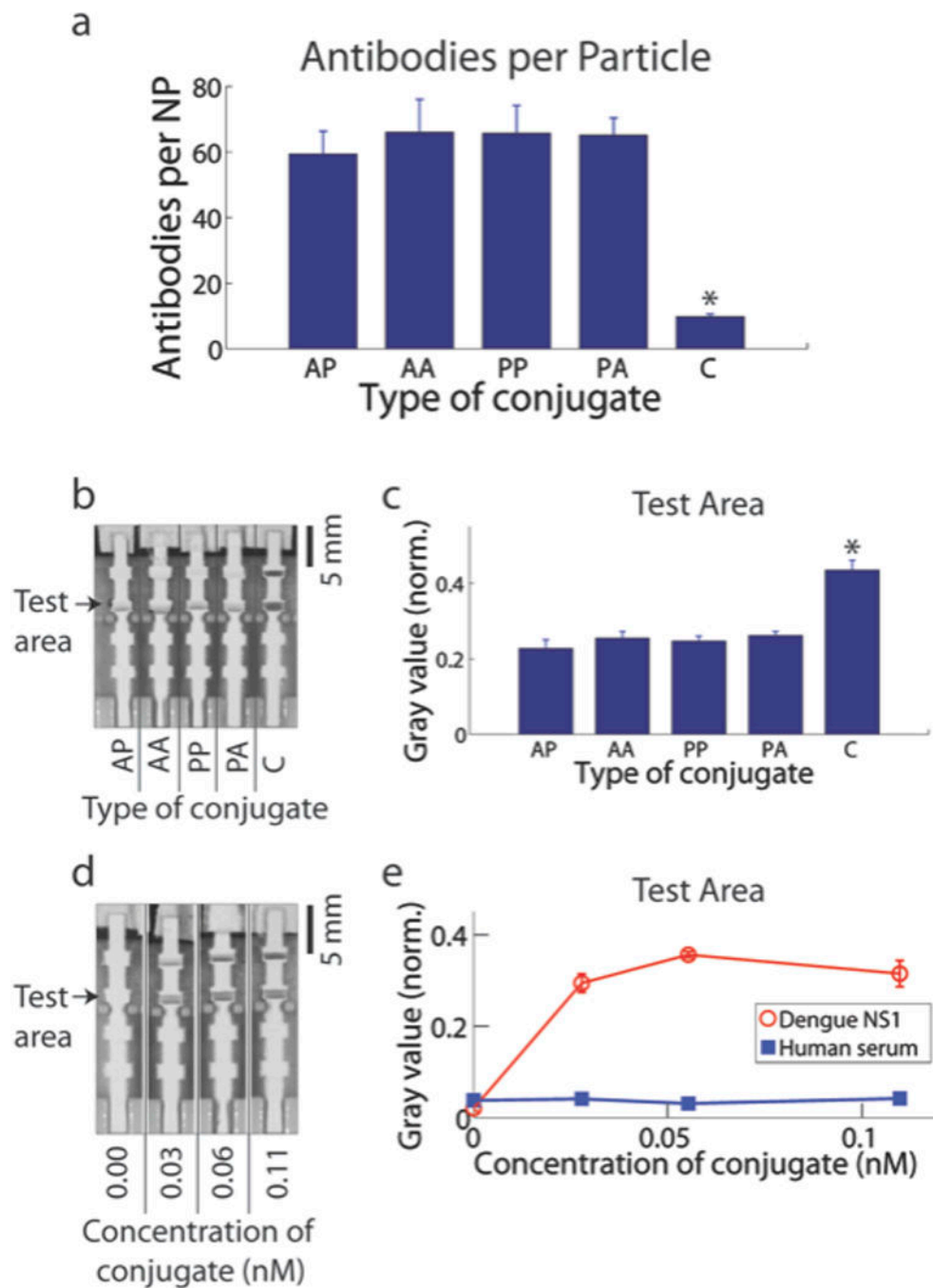


**Figure 3.** Evaluation of the effect of conjugation strategy on assay performance for fixed antibody concentration. (a) Antibody coverage on NPs. AA = active antibody conjugation, no mPEG-SH backfill. AP = active antibody conjugation, with mPEG-SH backfill. PA = passive antibody conjugation, no mPEG-SH backfill. PP = passive antibody conjugation with mPEG-SH backfill. C = Commercial NP-antibody conjugation. \* indicates  $p < 0.05$ , one-way ANOVA; (b) Test strips run with conjugates normalized by amount of antibodies. Sample is supernatant of Vero cells infected with Dengue Type 2 virus. Scale bar = 5 mm; (c) Image

analysis of (b); \* =  $p < 0.05$ , one-way ANOVA (d) Test strips run with increasing concentrations of conjugates, (e) Image analysis of (d).

Author Manuscript

Author Manuscript

Author Manuscript

Author Manuscript

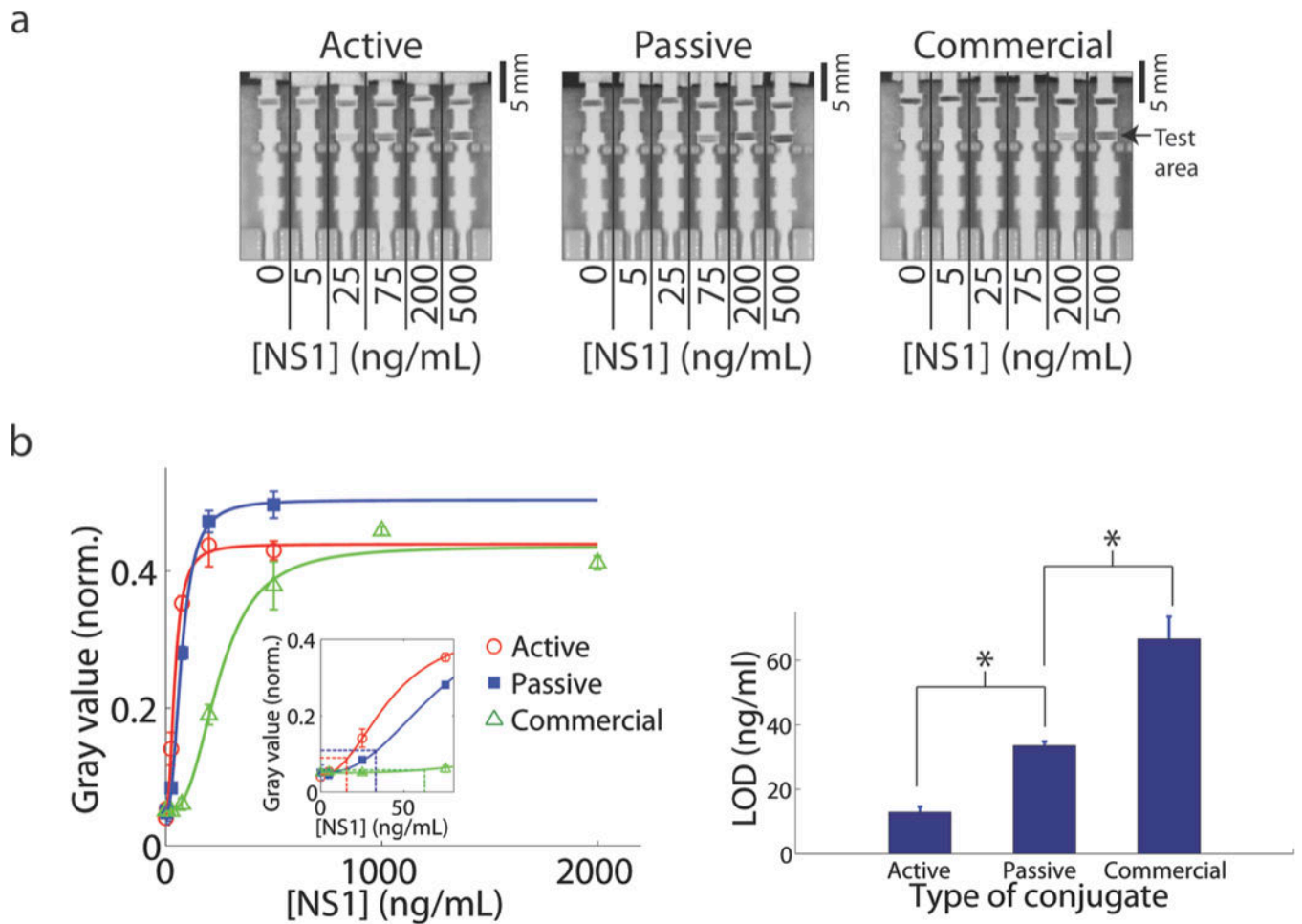


**Figure 4.** Evaluation of the effect of conjugation strategy on assay performance for fixed NP concentration. a) LOD measurement for active (left), passive (middle), and commercial (right) conjugation for 0.06 nM conjugate concentration, immobilized antibody at 0.4  $\mu\text{g}/\text{mm}$ , and serial dilution of purified Dengue NS1 in human serum. Scale bars = 5 mm. (b) Left, image analysis for active (red circles), passive (blue squares), and commercial conjugation (green triangles) with sigmoidal fits to calculate LOD values (dotted lines). Inset: zoom in for concentration 0–80 ng/ml. Right, Bar graph comparing LOD values from each conjugation.  $p < 0.001$ .

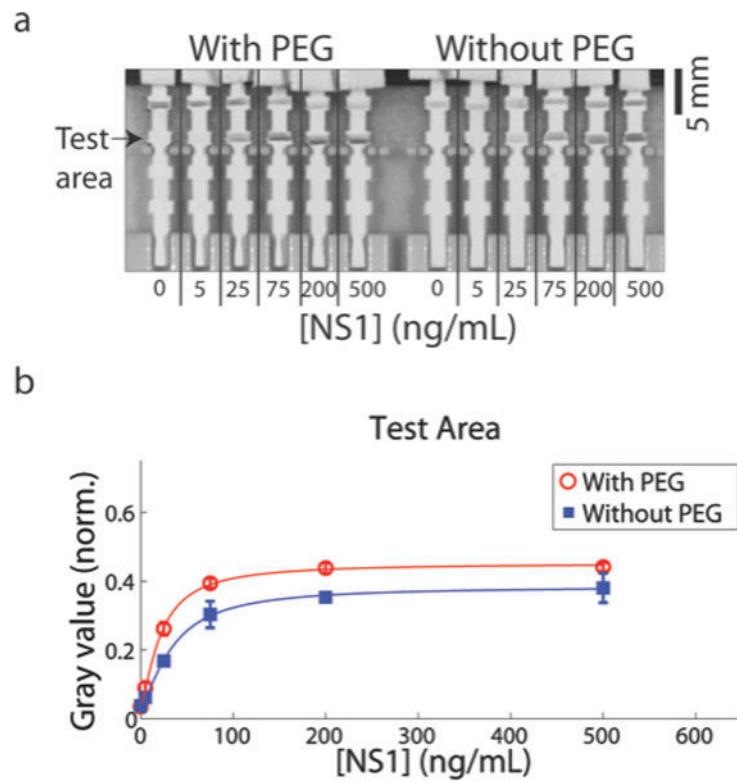


**Figure 5.** Effect of modifying the surface chemistry of NP-antibody conjugates. (a) Test strips prepared using active conjugates with (left) and without (right) PEG backfill. Scale bar = 5 mm; (b) Image analysis of test strips in images from (a).

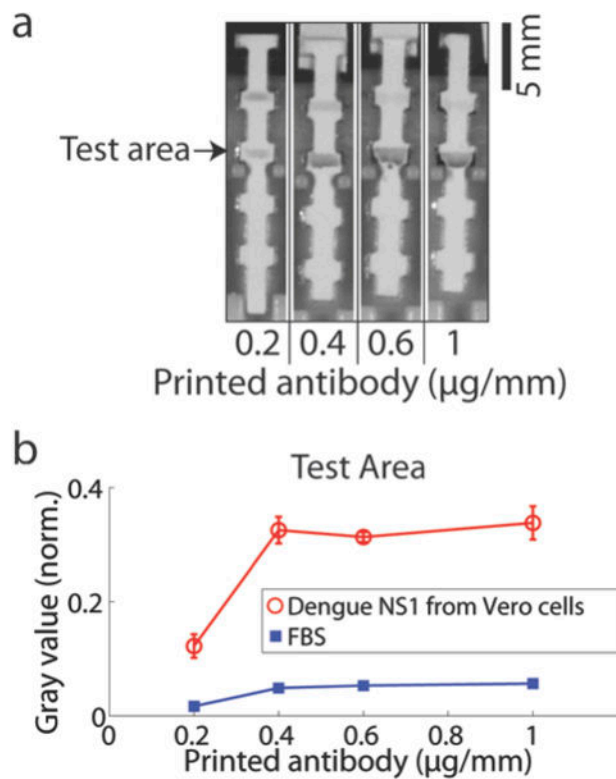


**Figure 6.** Effect of increasing stripes. (a) Strips run with increasing number of stripes of printed/immobilized antibody on the nitrocellulose. Scale bar = 5 mm. Tests for optimal printed antibody were run in duplicate. Control samples of human serum showed negligible background (Supplemental Fig. S3a,d). Control samples were run only once per stripe number. (b) Test line intensities from (a).

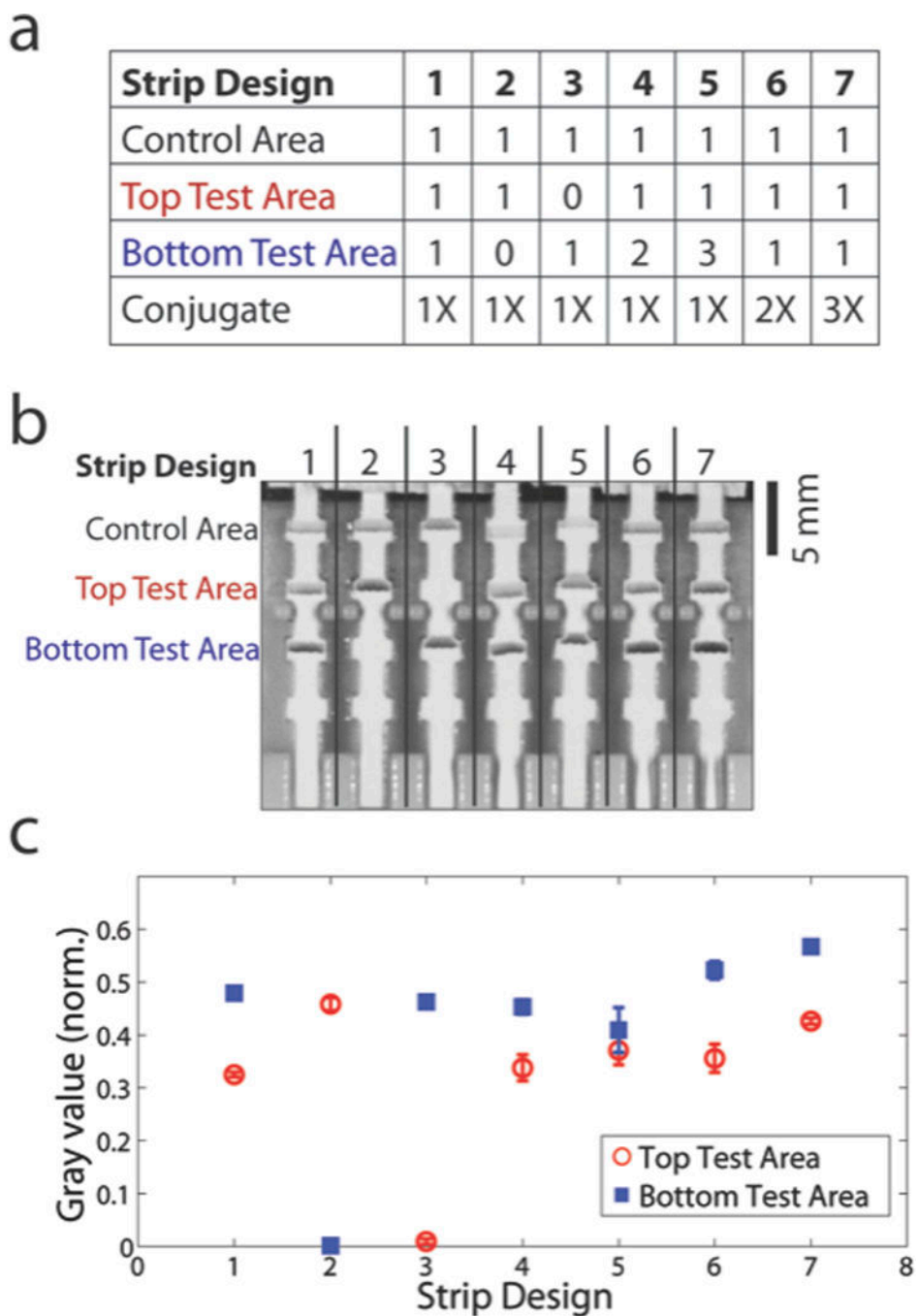


**Figure 7.** Effect of in-line multiplexing. a) Table of print numbers and NP-antibody concentrations for Strips Design 1–7. Table shows number of prints of immobilized antibody (Control and Test Areas) or concentration factor of conjugate. (b) Images of strips run with 40  $\mu$ l of supernatant of Vero cells infected with dengue type 2. Scale bar = 5 mm. (c) quantified test line intensities.